measured values of k_1. These are shown in Table IV as a function of temperature.

Examination of the data shown in Table IV indicates that over the temperature range which this study of the kinetics of the oxidation of nitrite was done the reverse reaction, the thermal decomposition of nitrate to form nitrate and oxygen could be ignored. It must be kept in mind, however, that at temperatures above 500 °C the value of k_{-1}, the reverse rate constant, begins to approach k_1 and this assumption is no longer valid.

Conclusion

We have shown that the principal intrinsic reaction in the equimolar binary $NaNO_3$–KNO_3 system over the temperature range 500–620 °C is the thermal decomposition of the nitrate ion to form nitrite and oxygen. The ratio of nitrate to nitrite has been shown to be proportional to $P_{O_2}^{1/2}$, indicating that this reaction scheme is unchanged as the oxygen partial pressure varies. Using the data from these experiments, we have been able to calculate the enthalpy, entropy, and free energy for this reaction. These data are in good agreement with similar thermodynamic data for the single salts.

The kinetics of the oxidation of nitrite in $NaNO_3$–KNO_3 have also been studied over the temperature range 400–500 °C. This reaction has been shown to be second order overall, first order with respect to both nitrite concentration and oxygen partial pressure. The implication of the first-order dependence on oxygen is that oxygen does not dissociate prior to reaction with nitrite. The activation energy for this reaction, calculated from the temperature dependence of the rate constants, was found to be 26.4 kcal/mol. Discrepancies in values of the forward rate constant between this work and earlier published studies were attributed to limitations on the oxidation rate imposed by mass transport of oxygen in the latter.

Acknowledgment. This work was supported by DOE under Contract DE-AC04-76D00789. The authors are indebted to D. L. Lindner for helpful discussions.

Registry No. KNO_3, 7757-79-1; $NaNO_3$, 7631-99-4; NO_3^-, 14797-55-8; NO_2^-, 14797-65-0.

Contribution from the Department of Chemistry, Texas A&M University, College Station, Texas 77843

1,4-Bis(2,5,5-tris(carboxymethyl)-2,5-diazapentyl)benzene (PXED3A): Synthesis, Binuclear Chelating Tendencies, and Iron(III) μ-Oxo Bridge Formation

CHIU YUEN NG,[1] ARTHUR E. MARTELL,* and RAMUNAS J. MOTEKAITIS

Received April 19, 1982

The synthesis of a new decadentate binucleating ligand 1,4-bis(2,5,5-tris(carboxymethyl)-2,5-diazapentyl)benzene (PXED3A, H_6L) and its aqueous equilibria with Cu(II), Co(II), Ni(II), Zn(II), Fe(II), and Fe(III) are described. At 25 °C and 0.100 M ionic strength, the logarithms of the protonation constants for PXED3A are 10.50, 9.83, 5.74, 4.77, 3.00, 2.29, 1.72, 1.2, ~0.9, and ~0.5. The logarithms of the formation constants $[ML]/[M][L]$ of the chelates having a 1:1 molar ratio of metal ion to ligand were found to be as follows: Cu(II), 18.0; Co(II), 15.88; Ni(II), 17.1; Zn(II), 15.93; Fe(II), 13.54. The 1:1 Fe(III) metal–chelate stability constant is estimated to be $10^{21\pm2}$ from the potentiometric data and the Fe(II)/Fe(III) redox potential. Stability constants of the protonated 1:1 chelates, MHL, MH_2L, MH_3L, and MH_4L, are also reported. The logarithms of the formation constants $[M_2L]/[M]^2[L]$ of binuclear chelates of divalent and trivalent metal ions were found to be as follows: Cu(II), 33.6; Co(II), 29.20; Ni(II), 23.2; Zn(II), 29.30; Fe(II), 25.38; Fe(III), 39.03. A spectrophotometric study of the Fe(III)–PXED3A system indicated formation of an intramolecular μ-oxo-bridged species above pH 3.5. Protonation constants for the 1:1 and 2:1 hydrolyzed complexes have also been determined. Probable ligand-bonding sites in the complexes are proposed, and their stabilities are compared with those formed from analogous chelating agents.

Introduction

Binuclear metal complexes have received considerable attention recently. By appropriate adjustment of the ligand backbone, a binucleating ligand is capable of coordinating two metal ions in such a way that both the distance and geometry between the two metal centers are suitable for binding of selected bridging molecules or anions. Binuclear complexes of this type can provide interesting models for studying catalytic reactions of biological systems in which concerted effects of both metal ions are involved.

Several types of binucleating ligands have been reported in the literature. Macrocyclic ligands having relatively rigid structures such as the cryptate compounds reported by Lehn and co-workers[2,3] and the binuclear "face-to-face" metalloporphyrins reported by Collman et al.,[4] in which metal ions are contained in a molecular cavity, provide high selectivity for metal ions and substrates. Another approach incorporates a rigid bridge such as a *p*- or *m*-xylene group in the ligand framework.[5-8] The metal–metal distance in these "wishbone" type binuclear complexes, first reported by Taqui Khan and Martell,[9] is such that a mono- or polyatomic bridging donor group can be bonded to both metal centers. Binuclear copper(I) complexes with a *p*-xylyl or *m*-xylyl backbone were reported to bind dioxygen reversibly[5-7] or to react with dioxygen to hydroxylate the xylyl ligand.[8] The present investigators reported the synthesis of a xylyl-bridged bis-terdentate

(1) Abstracted in part from a dissertation to be submitted by C.Y.N. to the Faculty of Texas A&M University in partial fulfillment of the requirements for the degree of Doctor of Philosophy.
(2) (a) Lehn, J. M.; Pine, S. H.; Watanabe, E.; Willard, A. J. *J. Am. Chem. Soc.* **1977**, *99*, 6766. (b) Lehn, J. M.; Sonveaux, I.; Willard, A. *Ibid.* **1978**, *100*, 4914.
(3) Martell, A. E.; Motekaitis, R. J.; Lecomte, J. P.; Lehn, J. M. submitted for publication in *Inorg. Chem.*
(4) Collman, J. P.; Denisevich, P.; Konai, Y.; Marrocco, M.; Koval, C.; Anson, F. C. *J. Am. Chem. Soc.* **1980**, *102*, 6027.
(5) Bulkowski, J. E.; Burk, P. L.; Ludman, M. F.; Osborn, J. A. *J. Chem. Soc., Chem. Commun.* **1977**, 498.
(6) Burk, P. L.; Osborn, J. A.; Youinou, M. T.; Agnus, Y.; Louis, R.; Weiss, R. *J. Am. Chem. Soc.* **1981**, *103*, 1273.
(7) Nisnida, Y.; Takahashi, K.; Kuramoto, H.; Kida, S. *Inorg. Chim. Acta* **1981**, *54*, L103.
(8) Karlin, K. D.; Dahlstrom, P. L.; Cozzette, S. N.; Scensny, P. M.; Zubieta, J. *J. Chem. Soc., Chem. Commun.* **1981**, 881.
(9) Taqui, Khan, M. M.; Martell, A. E. *Inorg. Chem.* **1975**, *14*, 676.

0020-1669/83/1322-0721$01.50/0

hexaamine[10] and measured the oxygenation constant of its cobalt(II) chelate.[11] As part of the continuing studies of the synthesis and properties of binuclear chelates, the investigation reported here describes the synthesis and metal complex equilibria of the *p*-xylyl-bridged bis-pentadentate polyamino acid 1,4-bis(2,5,5-tris(carboxymethyl)-2,5-diazapentyl)benzene (PXED3A, H_8L) (**1**).

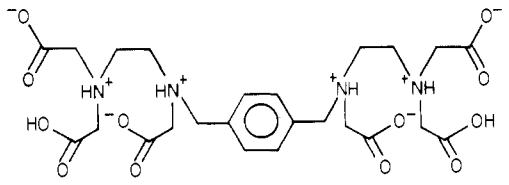

1 (PXED3A)

It is well-known that Fe(III) chelates of polyamino acids such as ethylenediaminetetraacetic acid (EDTA), *N*-(2-hydroxyethyl)-*N*,*N*′,*N*′-ethylenediaminetriacetic acid (HEDTA), and nitrilotriacetic acid (NTA) form stable μ-oxo dimers. These dimeric binuclear oxo-bridged Fe(III) complexes have been studied in detail and are well characterized.[12-19] Particular interest has been placed on the Fe–O–Fe structural unit since its properties provide useful information on some biologically important hemerythrin and other nonporphyrin iron–protein systems. This paper reports the coordination behavior of PXED3A with Fe(III) and the formation of a binuclear intramolecular μ-oxo-bridged Fe(III) complex.

Experimental Section

Ligand Synthesis. α,α'-Bis(ethylenediamino)-*p*-xylene Tetrahydrochloride. A mixture of *N*-acetylethylenediamine (10.2 g, 0.1 mol)[20] and 1,4-benzenedicarboxaldehyde (6.7 g, 0.05 mol) in 300 mL of methanol was heated for 15 min. The solution was hydrogenated at 3 atm over a 5% Pd on charcoal catalyst in a 2-L. Parr hydrogenation apparatus until the calculated amount of hydrogen was absorbed. The mixture was filtered, and the filtrate was concentrated with a rotary evaporator. Hydrochloric acid (200 mL, 6 M) was added to the resulting oil, the solution was refluxed for 2 days, and a colorless solid precipitated upon cooling. The product was collected and washed with cold ethanol. The NMR spectrum ($NaOD/D_2O$) showed three peaks at 2.58 (s), 3.66 (s), and 7.35 ppm (s) in the ratio of 2:1:1. Yield: 16.5 g (90%).

1,4-Bis(2,5,5-tris(carboxymethyl)-2,5-diazapentyl)benzene (1). α,α-Bis(*N*,*N*′-ethylenediamino)-*p*-xylene tetrahydrochloride (18.4 g, 0.050 mol) and bromoacetic acid (48.3 g, 0.350 mol) were dissolved in 200 mL of water, and the solution was kept at 50–55 °C. A 10 M NaOH solution was added dropwise with stirring so as to maintain the pH of the solution around 7. After 85 mL of 10 M NaOH was added, the volume of the solution was reduced and the inorganic salt was removed. The filtrate was then passed through a cation-exchange column (Dowex 50W-X8 in H^+ form) and was eluted with water. The strong-acid fraction was discarded, and the eluates were combined and concentrated under reduced pressure. The product precipitated when 200 mL of ethanol was added. The neutral ligand was obtained by recrystallization from a pH 1.5–2 solution. The NMR spectrum ($NaOD/D_2O$) showed five peaks at 2.60 (s), 3.03 (br s), 3.10 (s), 3.70 (s), and 7.33 ppm (s) in the ratio of 2:2:1:1:1. Yield: 11.4 g (40%). Anal. Calcd for $C_{24}H_4H_{34}O_{12}\cdot 2.2H_2O$: C, 47.28; H, 6.35; N, 9.19. Found: C, 47.17; H, 6.17; N, 9.39.

The more soluble pure ligand tetrahydrochloride was obtained by recrystallization from 2 N HCl and was used in potentiometric studies.

Reagents. Stock solutions of about 0.020 M of reagent grade metal nitrates were prepared in doubly distilled water, and their exact concentrations were determined by direct titration with previously standardized EDTA solution in the presence of appropriate indicators.[21] Carbonate-free solutions of 0.1000 M KOH were prepared from Dilut-it (R) ampules and standardized with potassium acid phthalate. Potassium nitrate, used as supporting electrolyte, was also obtained as reagent grade material. The 5% Pd/C catalyst was obtained from Engelhard, terephthaldehyde (98%) from Aldrich, and bromoacetic acid (practical grade) from Matheson Coleman and Bell.

Potentiometric Equilibrium Measurements. Potentiometric measurements of the ligand in the absence and presence of metal ions were carried out with a Beckman Research pH meter fitted with blue-glass and calomel reference electrodes and calibrated to read $-\log [H^+]$ directly. The temperature was maintained at 25.00 ± 0.05 °C, and the ionic strength was adjusted to 0.100 M by the addition of KNO_3.

The following procedure was employed for the measurement of Fe(II)–ligand solutions. A stoichiometric amount of analytical grade ferrous ammonium sulfate was placed in a small glass boat floating on the ligand solution, and the reaction system was deoxygenated for 1–2 h with an O_2- and CO_2-free nitrogen purge while the solution was stirred slowly. The stirrer was then speeded up to capsize the boat. After all of the ferrous ammonium sulfate was dissolved, small increments of carbonate- and oxygen-free 0.1000 M KOH solution were added and $\log [H^+]$ values were recorded.

The stability constant for the binuclear Fe(III) chelate, Fe_2L, was determined by measuring the Fe(III)/Fe(II) redox potential, by a modification of the potentiometric measurements described above. It was assumed that the "standard" potential does not vary and only the ratio of [Fe(III)]/[Fe(II)] varies. Also, all known equilibrium constants were taken into account in the calculations. Thus the extent of ligand protonation and all other equilibria were considered without simplifying assumptions. Under the conditions employed the Fe^{2+} ion exists only as the aquo ion. Although the work was done at low pH, the results apply to all pH values. In addition to the blue-glass and calomel electrodes, a Pt-sheet electrode (about 6 mm × 1 mm) was fitted into the titration cell. Various measured amounts of an Fe(III) salt and ligand were dissolved in solution, and the solution was purged with O_2- and CO_2-free nitrogen for 2 h. The redox potential was measured after capsizing a glass boat containing a measured amount of the Fe(II) salt into the solution. The pH of the solution was kept below 1.8 to avoid formation of iron(III) hydroxide. Simple aquo potentials of the Fe(III)/Fe(II) couple were measured under the same conditions to eliminate systematic errors by measuring six known Fe(III):Fe(II) ratios with 0.100 M HNO_3 and 0.100 M HCl media. Complexation of the anion was taken into account. The mean value found was −0.4964 ± 0.0004 V vs. the saturated calomel electrode at 25.0 °C.

Calculations. The proton association constants for PXED3A were calculated from potentiometric data with the program PKAS.[22] Metal chelate stability constants were calculated with the program BEST.[23]

The calculation of the 1:1 metal chelate stability constants was complicated somewhat by the fact that 5–10% of the ligand was taken up by the formation of binuclear chelates. Therefore, the preliminary 1:1 constants were calculated from the equilibrium data of the 1:1 systems by assuming that the formation constant for addition of a second mole of metal ion is 2–3 log units lower than the formation constants of the 1:1 chelates. The formation constants of the 2:1

(10) Ng, C. Y.; Motekaitis, R. J.; Martell, A. E. *Inorg. Chem.* **1979**, *18*, 2982.
(11) Ng, C. Y.; Martell, A. E.; Motekaitis, R. J. *J. Coord. Chem.* **1979**, *9*, 255.
(12) Gustafson, R. L.; Martell, A. E. *J. Phys. Chem.* **1963**, *67*, 576.
(13) Schugar, H.; Walling, C.; Jones, R. B.; Gray, H. B. *J. Am. Chem. Soc.* **1967**, *89*, 3712.
(14) Lippard, W. J.; Schugar, H. J.; Walling, C. *Inorg. Chem.* **1967**, *6*, 1825.
(15) Wilkins, R.; Yelin, R. *Inorg. Chem.* **1969**, *8*, 1470.
(16) Schugar, H.; Hubbard, A. T.; Anson, T.; Gray, H. B. *J. Am. Chem. Soc.* **1969**, *91*, 71.
(17) Walling, C.; Partch, R. J.; Weil, T. *Proc. Natl. Acad. Sci. U.S.A.* **1975**, *72*, 140.
(18) McLendon, G.; Motekaitis, R. J.; Martell, A. E. *Inorg. Chem.* **1976**, *15*, 2306.
(19) Motekaitis, R. J.; Martell, A. E.; Hayes, D.; Frenier, W. W. *Can. J. Chem.* **1980**, *58*, 1999.
(20) Aspinall, S. A. *J. Am. Chem. Soc.* **1941**, *63*, 852.
(21) Schwarzenbach, G.; Flaschka, H. "Complexometric Titrations", 2nd ed.; Methuen: London, 1969.
(22) Motekaitis, R. J.; Martell, A. E. *Can. J. Chem.* **1982**, *60*, 168.
(23) Motekaitis, R. J.; Martell, A. E., submitted for publication in *Can. J. Chem.*
(24) Smith, R. M.; Martell, A. E. "Critical Stability Constants"; Plenum: New York, 1974; Vol. 1; 1st suppl., Vol. 5, 1982.
(25) Smith, R. J.; Martell, A. E. "Critical Stability Constants"; Plenum: New York, 1975; Vol. 2; 1st suppl., Vol. 5, 1982.

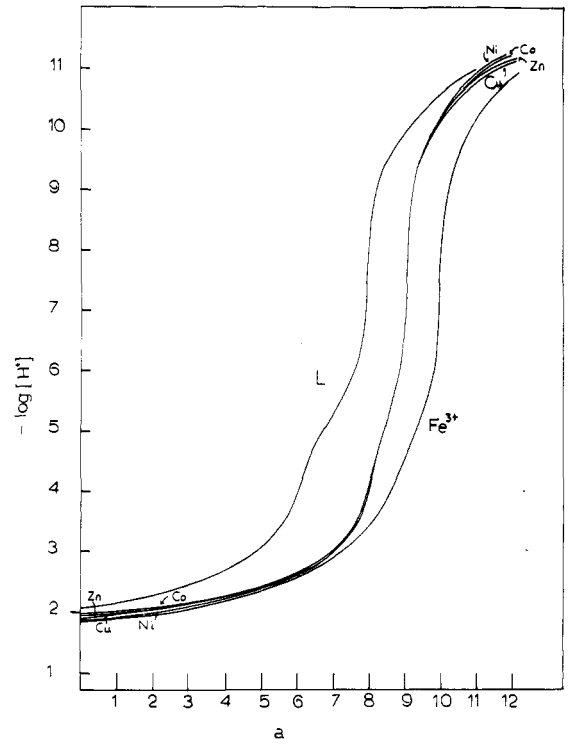

Figure 1. Potentiometric equilibrium curves of ligand alone L and 1:1 molar ratios of metal ion to PXED3A·4HCl as a function of added base, measured at 25 °C and μ = 0.100 M (KNO_3). In each case $[L]_T = 1.00 \times 10^{-3}$ M and a = moles of base per mole of PXED3A·4HCl.

chelates (M_2L) were then calculated with the inclusion of the K_{ML} and chelate deprotonation constants obtained from the 1:1 systems. A more detailed refinement of the preliminary constants of the 1:1 system was then carried out while including the formation constants of the binuclear chelates obtained from the 2:1 systems. The procedure was repeated without any simplifying approximations until the difference between the calculated and observed values of -log [H^+] were minimized for the potentiometric data of both the 1:1 and 2:1 chelates.

Computation of ϵ for the μ-Oxo Binuclear Fe(III) Chelates, Fe_2LO. The equilibrium constant for μ-oxo bridge formation is defined by

$$Fe_2(OH)_2L \overset{-H_2O}{\rightleftharpoons} Fe_2LO \qquad K_D = \frac{D}{X - D}$$

where D = molar concentration of Fe_2LO and X = total analytical concentration of the binuclear Fe(III) chelate. In terms of absorbance A at 475 nm where the absorbance of the FeLOH moieties is negligible, K_D becomes

$$K_D = \frac{A/\epsilon}{X - A/\epsilon}$$

The value of K_D was shown to be (vide supra) concentration independent but highly temperature dependent. If the heat of reaction is determined from the variation of log K_D with temperature, the following relationship applies:

$$\frac{dA}{d(1/T)} = \frac{\Delta H^\circ}{R} K_D \frac{X\epsilon}{1 + K_D}$$

It can be shown that there is only a unique value of ϵ that gives a linear plot of log K_D vs. $1/T$. Thus with the assumption that ΔH° is constant over the temperature range considered, both ϵ and ΔH° were obtained by a computer fit for the best straight line to measurements of absorbance with temperature.

Results

Protonation Constants. The potentiometric equilibrium curve of the tetrahydrochloride of PXED3A in the absence of metal ions is presented in Figure 1. The first inflection at a = 6 (where a is moles of base added per mole of ligand present in the experimental solution) corresponds to the neutralization of the six most acidic protons of the ligand, $H_{10}L^{4+}$. Of the six most acidic protonated donor groups, two are nearly completely dissociated in aqueous solution prior to the addition of base. The buffer regions studied extend from a = 0 to a = 10, with a sharp inflection at a = 8. Two more protons are released from a = 8 to a = 10. All deprotonation steps except for the first two were found to occur in a pH range in which dissociation constants may be calculated directly from potentiometric data. The log values of the proton association constants obtained, defined by eq 1 and 2 are listed in Table I together with those of analogous compounds[23] for comparison.

Table I. Protonation Constants of PXED3A and Analogous Ligands

	PXED3A[a]	HEDTA[b,c]	EDTA[b,d]	BED3A[b,e]
log K_1	10.50 (3)	9.81	10.17	9.84
log K_2	9.83 (2)			
log K_3	5.74 (1)	5.37	6.11	5.10
log K_4	4.77 (1)			
log K_5	3.00 (1)	2.6	2.68	1.9
log K_6	2.29 (1)			
log K_7	1.72 (3)			
log K_8	1.2			
log K_9	~0.9			
log K_{10}	~0.5			

[a] Present work; 25.0 °C; μ = 0.100 M (KNO_3). [b] Reference 24. [c] HEDTA = *N*-(2-hydroxyethyl)ethylenediamine-*N*,*N*',*N*'-triacetic acid. [d] EDTA = ethylenediaminetetraacetic acid. [e] BED3A = *N*-benzylethylenediamine-*N*,*N*',*N*'-triacetic acid.

$$H_{n-1}L^{(n-7)+} + H^+ \rightleftharpoons H_nL^{(n-6)+} \tag{1}$$

$$K^H_n = \frac{[H_nL^{(n-6)+}]}{[H_{n-1}L^{(n-7)+}][H^+]} \tag{2}$$

Mononuclear Chelates of Divalent Ions. The potentiometric equilibrium curves for the 1:1 molar ratio of metal ion to ligand shown in Figure 1 suggest strong interactions between the metal ions and PXED3A even at a = 0. The inflection at a = 8 indicates the formation of a diprotonated chelate MH_2L^{2-}. This is followed by a sharp inflection at a = 9 corresponding to the formation of a stable monoprotonated species MHL^{3-}, which then dissociates further at high pH. Additional protonated species are also found in the 1:1 systems at low pH. The equilibria describing the 1:1 system can be summarized by eq 3–5, and the equivalent sets of formation constants are defined by eq 6–8. The normal chelate formation constant,

$$M^{2+} + L^{6-} \rightleftharpoons ML^{4-} \tag{3}$$

$$MH_{n-1}L^{n-5} + H^+ \rightleftharpoons MH_nL^{n-4} \qquad n = 1\text{–}4 \tag{4}$$

$$M(OH)L^{5-} + H^+ \rightleftharpoons ML^{4-} \tag{5}$$

$$K_{ML} = \frac{[ML^{4-}]}{[M^{2+}][L^{6-}]} \tag{6}$$

$$K^H_{MH_nL} = \frac{[MH_nL^{n-4}]}{[MH_{n-1}L^{n-5}][H^+]} \qquad n = 1\text{–}4 \tag{7}$$

$$K^H_{ML} = \frac{[ML^{4-}]}{[M(OH)L^{5-}][H^+]} \tag{8}$$

K_{ML}, for Cu(II) and Ni(II) cannot be calculated accurately from the 1:1 potentiometric data, since the formation of the MH_4L species is almost complete even at the lowest pH measured. For this reason, the values of K_{ML} for Ni(II) and Cu(II) chelates were determined by ligand competition, involving the exchange equilibrium

$$ML + L' \rightleftharpoons ML' + L \tag{9}$$

Table II. Logarithms of Stability Constants of Metal Chelates of PXED3A[a]

	Co^{2+}	Zn^{2+}	Cu^{2+}	Ni^{2+}	Fe^{2+}	Fe^{3+}
K_{ML}	15.88 (5)	15.93 (5)	18.0 (2)	17.1 (1)	13.54 (2)	
K^{H}_{MHL}	9.80 (3)	9.79 (3)	10.02 (3)	9.78 (3)	9.81 (2)	31.53 (4)[b]
$K^{H}_{MH_2L}$	4.98 (3)	4.99 (3)	5.20 (3)	5.12 (2)	5.28 (2)	4.91 (4)
$K^{H}_{MH_3L}$	2.49 (2)	2.45 (2)	2.67 (3)	2.30 (2)	2.99 (1)	2.34 (4)
$K^{H}_{MH_4L}$	2.05 (2)	2.17 (3)	2.21 (2)	1.95 (3)	2.23 (3)	1.5 (1)
K^{H}_{ML}	11.2 (1)	10.9 (1)	10.6 (1)	11.1 (1)	11.42 (5)	
$K^{H}_{M(OH)L}$						11.06 (5)
$K^{M}_{M_2L}$	13.30 (6)	13.40 (6)	15.6 (1)	15.2 (1)	11.84 (4)	39.03 (6)[c]
$K^{H}_{M_2HL}$	2.35 (4)	2.20 (4)	2.80 (4)	2.50 (5)	2.57 (2)	0.7 (1)
$K^{H}_{M_2L}$	10.5 (1)	10.2 (1)	10.1 (1)	10.6 (1)	10.82 (4)	2.67 (6)
$K^{H}_{M_2(OH)L}$			11.2 (1)			3.70 (5)

[a] $T = 25.0$ °C; $\mu = 0.100$ M (KNO_3). [b] $\beta_{MHL} = [MHL]/[M][L][H]$. [c] $\beta_{M_2L} = [M_2L]/[M]^2[L]$; $K_{ML} = [ML]/[M][L]$; $K^{H}_{MH_nL} = [MH_nL]/[MH_{n-1}L][H]$; $K^{H}_{M(OH)_{n-1}L} = [M(OH)_{n-1}L]/[M(OH)_nL][H^+]$; $K^{M}_{M_2L} = [M_2L]/[ML][M]$; $K^{H}_{M_2HL} = [M_2HL]/[M_2L][H]$; $K^{H}_{M_2(OH)_{n-1}L} = [M_2(OH)_{n-1}L]/[M_2(OH)_nL][H^+]$.

Tris(2-aminoethyl)amine trihydrochloride (tren·3HCl) was used as the competing ligand in the copper(II) system, whereas bipyridine (bpy) was chosen for the nickel(II) determination.

In the Cu(II)–tren–PXEDA3A system, with a 1:1:1 molar ratio of constituents, Cu(II) is completely coordinated with PXED3A at low pH, and displacement by tren occurs only above pH 8. In the case of Ni(II), with a 1:3:1 molar ratio of Ni(II):bpy:PXED3A, the tris(bipyridyl) chelate is the dominant species at low pH, and conversion to the PXED3A chelate occurs as the pH is increased to about 7. The formation constants obtained from these ligand-exchange measurements are presented in Table II. Ligand protonation and chelate formation constants of tren and bpy with the appropriate metal ions were taken from the literature.[24,25] As an added check, the protonation constants and chelate formation constants were measured for tren, bpy, and the appropriate metal ions, under the conditions employed in this research. The results obtained were found to be in agreement with literature values.

Binuclear Chelates of Divalent Metal Ions. Potentiometric equilibrium curves for systems containing a 2:1 molar ratio of metal ion to ligand, shown in Figure 2, have a long low-pH buffer region followed by a sharp inflection at $a = 10$, corresponding to complete formation of the 2:1 chelates, M_2L^{2-}. The high-pH buffer region that follows the inflection corresponds to the formation of hydroxo chelates. It was also determined from the potentiometric data that all binuclear chelates of the divalent metal ions form monoprotonated complexes. The ligand solution equilibria for binuclear chelate formation are shown as eq 10–12. The equilibrium formation constant set is defined in eq 13–15. The values calculated for the stability constants of the binuclear chelates are listed in Table II.

$$ML^{4-} + M^{2+} \rightleftharpoons M_2L^{2-} \quad (10)$$

$$M_2L^{2-} + H^+ \rightleftharpoons M_2HL^- \quad (11)$$

$$M_2(OH)L^{3-} + H^+ \rightleftharpoons M_2L^{2-} \quad (12)$$

$$K^{M}_{M_2L} = \frac{[M_2L^{2-}]}{[ML^{4-}][M^{2+}]} \quad (13)$$

$$K^{H}_{M_2HL} = \frac{[M_2HL^-]}{[M_2L^{2-}][H^+]} \quad (14)$$

$$K^{H}_{M_2L} = \frac{[M_2L^{2-}]}{[M_2(OH)L^{3-}][H^+]} \quad (15)$$

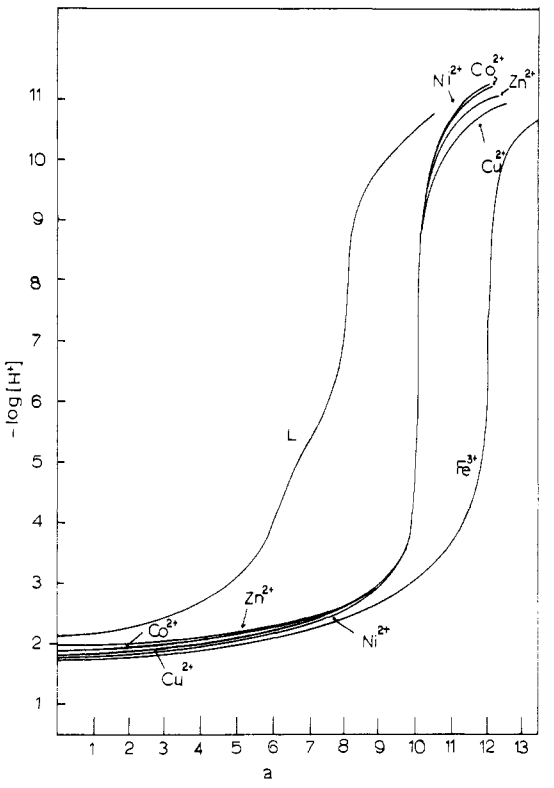

Figure 2. Potentiometric equilibrium curves of ligand alone L and 2:1 molar ratios of metal ion to PXED3A·4HCl as a function of added base, measured at 25 °C and $\mu = 0.100$ M (KNO_3). In each case $[L]_T = 1.00 \times 10^{-3}$ M and a = moles of base per mole of PXED3A·4HCl.

Fe(III)–PXED3A System. Potentiometric equilibrium curves having 1:1 and 2:1 molar ratios of metal ion to ligand are shown in Figures 1 and 2, respectively. For the 2:1 system the strong inflection at $a = 12$ indicates 2 mol of hydrogen ion was neutralized in addition to the 10 mol released from the ligand. The 2:1 chelate formation constant, β_{M_2L}, cannot be calculated directly from the titration curve since total complexation of Fe(III) with the ligand molecule is complete even at very low pH. The β_{M_2L} constant (eq 16) was therefore determined from the reduction potential measurement described in the Experimental Section. Moreover, two stepwise protonation constants of the 2:1 hydroxo chelates, illustrated by eq 17 and 18, were obtained from the potentiometric equilibrium data. The constants obtained, defined by eq 19–21, are shown in Table II. Aqueous solutions of the 2:1

$$2M^{3+} + L^{6-} \rightleftharpoons M_2L \quad (16)$$

$$M_2(OH)L^- + H^+ \rightleftharpoons M_2L \quad (17)$$

$$M_2(OH)_2L^{2-} + H^+ \rightleftharpoons M_2(OH)L^- \quad (18)$$

$$\beta_{M_2L} = \frac{[M_2L]}{[M^{3+}]^2[L^{6-}]} \quad (19)$$

$$K^H_{M_2L} = \frac{[M_2L]}{[M_2(OH)L^-][H^+]} \quad (20)$$

$$K^H_{M_2(OH)L} = \frac{[M_2(OH)L^-]}{[M_2(OH)_2L^{2-}][H^+]} \quad (21)$$

Fe(III)–PXED3A chelate have a deep orange-red color above pH 3.5. The visible spectrum of this orange-red solution at pH 9, shown in Figure 3, is very similar to the spectra of the μ-oxo dimers of the 1:1 Fe(III)–EDTA[19] and Fe(III)–HEDTA[13] systems, and the absorbance peak at 475 nm is therefore attributed to the presence of an oxo-bridged binuclear Fe(III) complex. For a determination of the concentration dependence of the formation of the oxo-bridged Fe(III) complex, a series of 2:1 Fe(III)–PXED3A solutions was prepared with a wide range of concentration and the pH of the solutions was adjusted to pH 9. A plot of optical density at 475 nm vs. total Fe(III) concentration, Figure 4, shows adherence to Beer's law. A similar plot of absorptivity at 475 nm vs. total Fe(III) concentration of 1:1 Fe(III)–HEDTA solutions containing the binuclear μ-oxo complex shows considerable deviation from linearity over the same concentration range. The monomeric nature of the binuclear Fe(III)–PXED3A oxo complex is strongly indicated by the linear relationship of absorption vs. concentration, and the oxo bridge is therefore considered to form between two Fe(III) ions within the same molecule. The following equations apply:

$$Fe_2(OH)_2L \overset{K_D}{\rightleftharpoons} Fe_2LO \quad (22)$$

$$K_D = \frac{[Fe_2LO]}{[Fe_2(OH)_2L]} \quad (23)$$

For a determination of the intramolecular equilibrium constant, K_D, either the concentration of the dihydroxy chelate or the concentration of the μ-oxo binuclear complex must be measured.

The concentration of the μ-oxo binuclear complex can be followed easily from the intensity of the 475-nm band provided that the molar extinction coefficient is known. In an attempt to determine the molar extinction coefficient at 475 nm, a plot of absorbance vs. temperature was carried out (it is assumed that, below a certain temperature, the solution is composed of virtually 100% of μ-oxo complex and the absorbance would level off). However, the plot yielded a straight line extending from +90 to −10 °C. No attempt was conducted to measure the absorbance below −10 °C. The extinction coefficient determination was therefore based on the temperature dependence of oxo bridge formation in accordance with the method described for the Fe(III)–EDTA system.[19] Plots of log K_D vs. reciprocal of temperature were constructed with various assumed values of ϵ for the calculation of K_D at each temperature. The ϵ that gave the best straight line was then taken as the extinction coefficient for the 475-nm absorption band. The linear requirement for ϵ is justified in the Experimental Section. By this method, the molar extinction coefficient was found to be 180 M^{-1} cm^{-1}. The ΔH of oxo bridge formation was calculated from the slope of the plot, shown

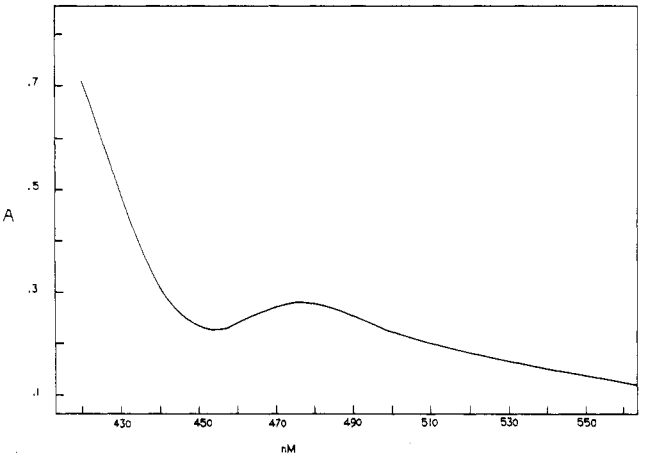

Figure 3. Visible absorption spectrum of the 2:1 Fe(III)–PXED3A chelate at pH 9.00, $[L]_T = 2.4 \times 10^{-3}$ M, $[Fe(III)]_T = 4.8 \times 10^{-3}$ M, $\mu = 0.100$ M (KNO_3), and $t = 25$ °C.

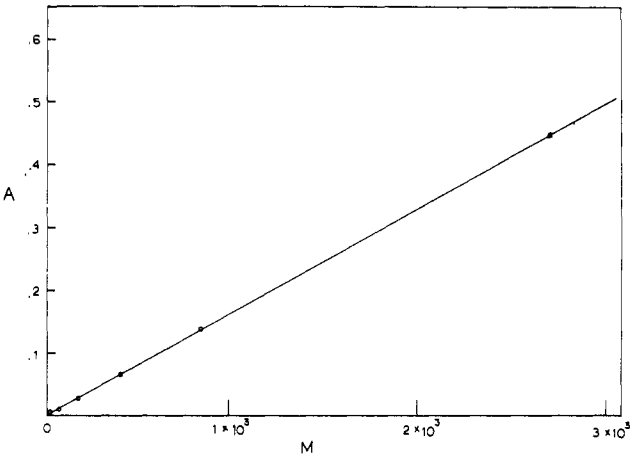

Figure 4. Plot of optical density at 475 nm vs. concentration of the Fe(III)–PXED3A 2:1 chelate at pH 9.0, $t = 25$ °C, and $\mu = 0.100$ M (KNO_3).

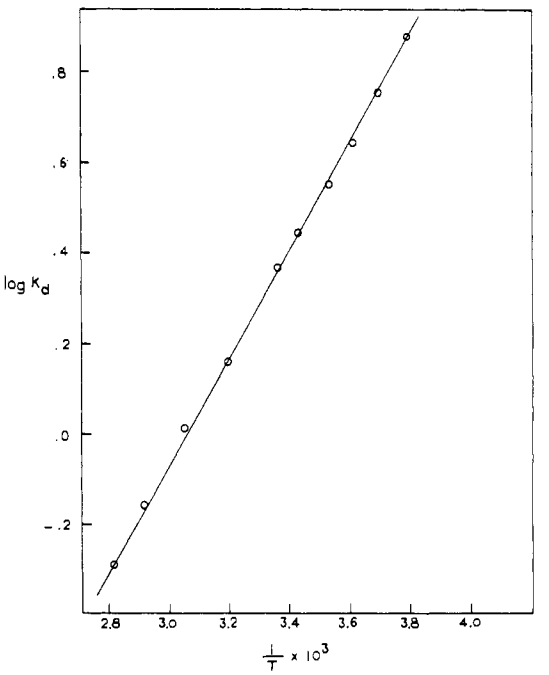

Figure 5. Plot of log K_D vs. $1/T$ ($K_D = [Fe_2LO^{2-}]/[Fe_2(OH)_2L^{2-}]$; T = K). From the slope $\Delta H = -5.4$ kcal/mol; from the intercept $\Delta S = -16.5$ eu.

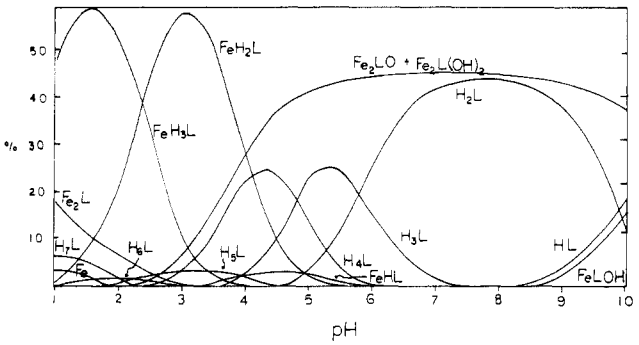

Figure 6. Species distributions in the 1:1 Fe(III)–PXED3A system as a function of –log $[H^+]$ at $[L]_T = [M]_T = 10^{-3}$ M and $\mu = 0.100$ M (KNO_3).

in Figure 5, and was found to be –5.4 kcal mol^{-1}. The intercept yielded $\Delta S° = -16.5$ eu.

The inflection in the 1:1 curve (Figure 1) occurs at $a = 10$. The 1:1 solution is orange-red at the inflection. If it is assumed that the 1:1 Fe(III)–PXED3A chelate reacts in a manner analogous to those described above for the divalent metal ions, the inflection at $a = 10$ may be interpreted as the formation of a monohydroxy monoprotonated chelate $Fe(OH)HL^{3-}$ or a 1:1 chelate FeL, without coordinated hydrogen and hydroxide ions, which are indistinguishable. However, a species analysis of the 1:1 system with the equilibrium constants obtained from the 2:1 system reveals a different picture (Figure 6). Protonated chelates are the major species at low pH. As the pH rises, 1:1 chelates disproportionate into free ligand and the binuclear dihydroxo complex $Fe_2(OH)_2L^{2-}$, together with the μ-oxo-bridged complex Fe_2LO^{2-}. At pH 8, corresponding to the inflection in the 1:1 potentiometric equilibrium curve (Figure 1), Fe_2LO^{2-}, $Fe_2(OH)_2L^{2-}$, and H_2L^{4-} are the only dominant species in the solution. The visible spectrum of the 1:1 solution taken above pH 8 is identical with that of the 2:1 solution, with the absorbance at 475 nm about half the intensity of that of the 2:1 system. The fact that 10 mol of base/mol of ligand was neutralized at the inflection can be readily accounted for by the following: (1) six protons were released in the formation of 0.5 mol of μ-oxo and dihydroxy 2:1 complexes, corresponding to an inflection in the 2:1 equilibrium curve at $a = 12$; (2) four additional protons were neutralized to give 0.5 mol of H_2L, corresponding to the inflection in the ligand curve (pH 7–9) at $a = 8$. It is not possible to calculate the formation constant of the 1:1 Fe(III)–PXED3A chelate from the equilibrium data since the concentration of the 1:1 chelate was negligible throughout the whole pH range as shown in Figure 6.

Discussion

Ligand Protonation Constants. The basicities of the ligand donor groups may be compared with those of the analogous polyamino acids HEDTA, EDTA, and *N*-benzylethylenedinitrilo-*N*,*N*′,*N*′-triacetic acid (BED3A). The first protonation step in HEDTA takes place on one of the amino nitrogens. With a positive charge on the molecule, Coulombic repulsion greatly reduces the protonation tendency for the second amino group. This effect is best illustrated quantitatively in the relative magnitudes of the first two protonation constants of HEDTA, $10^{9.81}$ and $10^{5.37}$. The ligand involved in this investigation, PXED3A (**1**), contains two widely separated pentadentate moieties. Thus the stepwise addition of protons to the PXED3A molecule can be envisioned as proceeding through the successive protonation of two separate ethylenediaminetriacetic acid molecules. Since the first two protons added to the ligand will be well separated from each other by the xylyl bridge, K^H_1 and K^H_2 decrease monotonically, reflecting only an increase in two widely separated positive charges so that the pK difference approaches the statistically controlled value. For the addition of the third and the fourth protons, charge repulsion becomes the dominant factor in lowering the basicity of the two remaining nitrogens in the molecule. The successive values for the protonation constants for carboxylate groups may also be rationalized in a similar fashion.

Metal Chelate Stability Constants for the Divalent Metal Ions. Although PXED3A is formally a decadentate ligand, the rigid *p*-xylene bridge precludes the participation of all donor groups in mononuclear 1:1 complexation. Thus, each combination of five donor groups at each end of the molecule can best be regarded as individual pentadentate ligands. Consequently, the 1:1 chelate formation constants of PXED3A and divalent metal ions are of the same order of magnitude as those of the pentadentate ligands HEDTA and BED3A and are much lower than those of the higher polyamino polycarboxylic acids such as diethylenetriaminepentaacetic acid (DTPA) and triethylenetetraminehexaacetic acid (TTHA). Thus the basicity of the uncoordinated end of the 1:1 chelate is not expected to be greatly affected by the presence of the metal chelate because of the large intergroup distance required by the α,α'-xylene bridge. In fact, chelate protonation constants for all the divalent metal 1:1 chelates are similar in magnitude. The values of these constants fall between those of the corresponding ligand protonation constants: e.g., the values of K^H_{MHL} vs. K_1 and K_2 etc. are quite comparable to the protonation constants of analogous ligands, HEDTA, BED3A, and EDTA.

For systems in which two metal ions are equilibrated with one ligand, the M_2L species become dominant even at low pH. Since the two metal centers are far apart, Coulombic repulsion between the two metal ions does not play a significant role in the formation of the 2:1 complexes. The stepwise 2:1 formation constants are only 1–2 log units smaller than the 1:1 constants. The decrease in stability can be related to the lowering of basicities of the "free" end when a metal ion is coordinated to the ligand.

Hydrolysis of the 1:1 metal chelate of PXED3A occurs at a higher pH than the corresponding reactions of HEDTA and EDTA. This behavior may be attributed to the high basicity of the monoprotonated chelate MHL of PXED3A. Unlike EDTA and HEDTA, where formation of the total deprotonated chelate occurs at much lower pH, a substantial concentration of the ML species of PXED3A appears only at approximately pH 10 after deprotonation of the MHL chelate. Subsequent formation of the M(OH)L species can only take place at higher pH. The hydrolysis constant for the microspecies M(OH)LH of PXED3A, in which a hydroxyl anion is bonded to the pentacoordinated metal ion with the proton on the uncoordinated end of PXED3A, may be of the same order of magntiude as the hydrolysis constants reported for HEDTA and EDTA chelates. It is of course impossible to distinguish between the microspecies M(OH)LH and ML from the potentiometric data.

Fe(III)–PXED3A System. The 2:1 PXED3A–Fe(III) stability constant, determined through the use of Fe(III)/Fe(II) potential, was found to be $10^{39.03}$. Compared with the 2:1 complexes of divalent metal ions, the more stable Fe(III) chelate has much lower proton affinity and lowers the value of $K^H_{M_2HL}$ by more than 1 log unit. The 1:1 Fe(III)–PXED3A formation constant cannot be calculated from the potentiometric data because it is not formed in appreciable concentration under reaction conditions employed. However, if the difference between the 1:1 and 2:1 stepwise formation constants were assumed to be within 2–3 log units, as is the case of other metal ions, the value of K_{ML} can be estimated to be $10^{21\pm2}$. The 1:1 hydroxy chelate protonation constant can

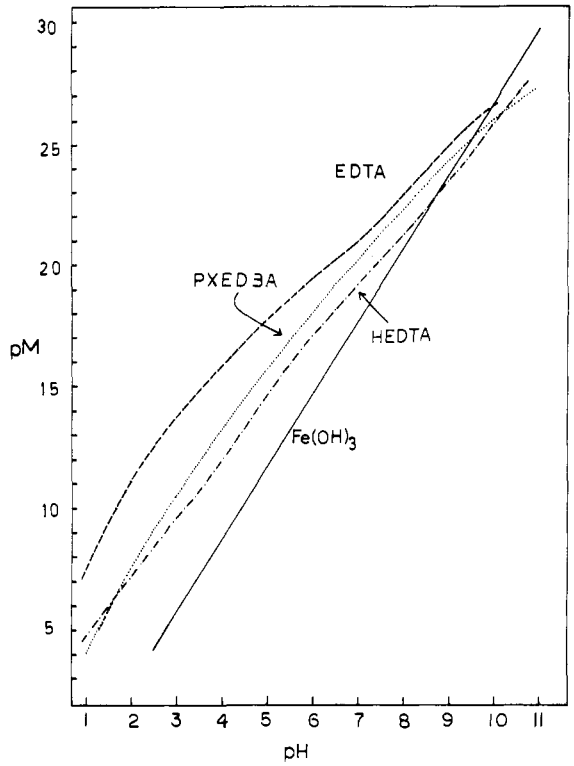

Figure 7. Plot of pM (-log $[Fe^{3+}]$) vs. pH (-log $[H^+]$): (---) $[Fe^{3+}]_T$ = 0.001 00 M, $[EDTA]_T$ = 0.001 10 M; (···) $[Fe^{3+}]_T$ = 0.001 00 M, $[PXED3A]_T$ = 0.001 10 M; (-·-·-) $[Fe^{3+}]_T$ = 0.001 00 M, $[HEDTA]_T$ = 0.001 10 M.

therefore be estimated to be about 10^4, quite similar to the value of $10^{3.9}$ given for the analogous Fe(III)–HEDTA complex. Further support for this approximation comes from the hydrolysis constants of the 2:1 complexes. The protonation constants of $M_2(OH)L$ and $M_2(OH)_2L$ are on the order of 10^3–10^4, which is in good agreement with the corresponding hydrolysis constant for MLOH.

The relative binding effectiveness of iron(III) by EDTA, PXED3A, and HEDTA can be demonstrated by a plot of pM (-log $[Fe^{3+}]$) vs. pH. A larger pM value indicates a more stable Fe(III) chelate. As shown in Figure 7, the values of pM for the 1:1 Fe(III) systems of EDTA, PXED3A, and HEDTA are in the decreasing order EDTA > PXED3A > HEDTA, over a wide pH range. This result indicates that the ability of PXED3A to complex Fe^{3+} ions falls between EDTA and HEDTA, which is consistent with the stability data presented above.

One of the more interesting properties of the 2:1 Fe(III)–PXED3A chelate is its ability to form an intramolecular μ-oxo-bridged complex. The monomeric nature of the μ-oxo complex is clearly demonstrated by the plot of the optical density of the μ-oxo-complex solution at 475 nm vs. the concentration of the 2:1 Fe(III)–PXED3A chelate. The linear nature of the plot over a wide range of concentrations indicates that the μ-oxo-complex solution obeys Beer's law. The intramolecular character of the Fe(III)–PXED3A μ-oxo dimer is also reflected by the hydrolysis and μ-oxo cyclization constants listed in Table III. Compared with Fe(III)–HEDTA and Fe(III)–EDTA chelates, the 2:1 Fe(III)–PXED3A complex shows a somewhat stronger tendency for hydrolysis but a considerably weaker tendency for internal oxo bridge formation. For the Fe(III)–PXED3A chelate, steric effects and a less than optimal Fe(III)–Fe(III) distance may be an important factor in the formation of oxo-bridged species. Since the two Fe(III) centers in the Fe(III)–PXED3A chelate cannot approach each other as freely as is the case for the mononuclear Fe(III)–HEDTA and Fe(III)–EDTA complexes, oxo bridge formation therefore proceeds to a much lesser extent in the case of the Fe(III)–PXED3A system.

Table III. Logarithms of Equilibrium Constants for Hydrolysis and Binuclear Chelate Formation for Iron(III) Chelates of PXED3A and Analogous Ligands

equilibrium quotient	Fe(III)–PXED3A[a]	Fe(III)–HEDTA	Fe(III)–EDTA
[ML]/[M][L]	(21 ± 2)	19.8[c]	25.0[c]
[ML]/[M(OH)L][H⁺]	(3.9 ± 1)	3.9[b]	7.5[c]
[ML(OH)L]/[M(OH)₂L][H⁺]	11.0	8.8[c]	
[M₂L]/[M₂(OH)L][H⁺]	2.9		
[M₂(OH)L]/[M₂(OH)₂L][H⁺]	3.7		
K_D	0.3[e]	2.3[b]	2.9[b]
ΔH, kcal mol⁻¹	−5.4	−7.1[d]	−15.0[b]
ΔS, eu	−16.5	−13.0[d]	−36[b]

[a] This work. [b] References 12. [c] Reference 24. [d] Reference 13. [e] Dimensionless; all other units for constants in the table are M^{-1}.

Although the oxo bridge formation constant K_D of Fe(III)–PXED3A chelate is much smaller than the K_D of Fe(III)–EDTA and Fe(III)–HEDTA, the difference in the magnitudes of the constants is not indicative of the relative degree of μ-oxo complex formation in these systems. For Fe(III)–EDTA and Fe(III)–HEDTA, μ-oxo bridge formation is highly concentration dependent, since the reaction involves the association of two mononuclear chelates. On the contrary, conversion of the dihydroxo complex of 2:1 Fe(III)–PXED3A to the intramolecular μ-oxo complex is independent of concentration. For example, in a 0.10 M Fe(III)–EDTA solution at 25.0 °C and pH 9.5, 92% of the chelate is in the form of μ-oxo dimer. However, if the concentration of the solution is lowered to 0.0010 M, only 46% of the chelate is dimerized. In the case of Fe(III)–PXED3A, under the same conditions, the ratio of μ-oxo complex (Fe_2LO to dihydroxo complex $Fe_2L(OH)_2$ remains 70% to 30% regardless of the concentration of the solution.

The absence of measurable concentration of intermolecular dimer can be ascribed tentatively to entropy effects. The presence of two hydroxo–Fe(III) moieties attached to the same backbond provides an effective local concentration of Fe–OH to Fe–OH of something approaching 1 M, while the actual concentration is only 30% (70% Fe–O–Fe) of the original molarity. These facts taken with an increased steric (ill-defined) barrier couple to give the results found: only intramolecular μ-oxo cyclization.

The effect of temperature on the dimerization equilibrium is considerably less for Fe(III)–PXED3A than for the analogous Fe(III)–EDTA and Fe(III)–HEDTA systems. A plot of concentrations of the intramolecular μ-oxo complex and the dihydroxy chelate as a function of temperature for a 0.0100 M 2:1 Fe(III)–PXED3A solution (Figure 8) shows that the concentration of the μ-oxo dinuclear complex decreases nearly linearly as the temperature is raised. At 55.5 °C, the two species are of equal molarity in solution. For a similar Fe(III)–EDTA solution μ-oxo-dimer concentration decreases more rapidly with increasing temperature. At 100 °C, only 1% of the Fe(III)–EDTA is in the form of the μ-oxo dimer[19] compared with 22% oxo-bridged species for Fe(III)–PXED3A.

The μ-oxo complex of Fe(III)–PXED3A chelate is very stable at high pH, while the μ-oxo-dimer solution of Fe(III)–HEDTA starts to decompose at pH values above 9, as evidenced by the disappearance of the orange-red color of the solution. The intensity of the absorption band of the Fe(III)–PXED3A μ-oxo complex remains unaltered as the pH is raised, until precipitation of $Fe(OH)_3$ occurs at about pH 10.

In view of the strain imposed by the structure of the ligand, the Fe–O–Fe angle in the Fe(III)–PXED3A μ-oxo complex

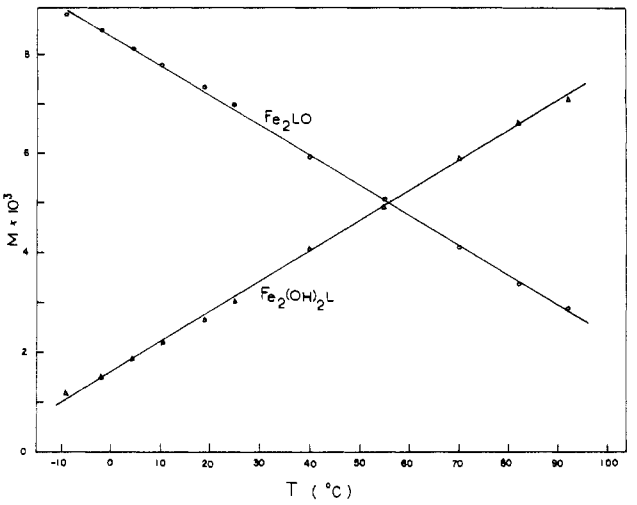

Figure 8. Concentrations of the intramolecular μ-oxo complex, Fe_2LO (L = PXED3A), and the dihydroxy chelate, $Fe_2(OH)_2L$, plotted as a function of temperature at $[Fe^{3+}]_T$ = 0.0200 M, $[PXED3A]_T$ = 0.0100 M, and pH 9.30.

probably deviates appreciably from the ideal 180° generally observed in other M–O–M systems.[26] Crystal structures of several μ-oxo Fe(III) complexes containing O and N donor groups[13,27,28] were also reported to have nonlinear Fe–O–Fe angles. The characteristic orange-red color, of the Fe(III)–PXED3A μ-oxo complex, has a molar extinction coefficient at 475 nm of 180, which is similar in magnitude to those reported for the analogous μ-oxo dimers of Fe(III)–HEDTA and Fe(III)–EDTA.[13,19] Although no evidence has been provided in this work on the structure of the Fe(III)–PXED3A μ-oxo chelate, the stoichiometry of complex formation, the equilibrium constants involved, and the electronic absorption spectrum indicate that the most reasonable structure of the μ-oxo dimer is that indicated schematically by formula **2**.

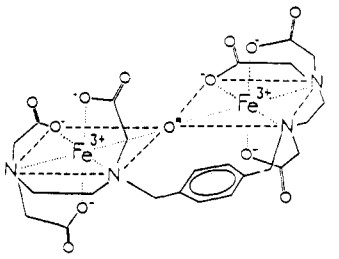

2

Acknowledgment. This research was supported by Grant A-259 from the Robert A. Welch Foundation.

(26) Murray, K. S. *Coord. Chem. Rev.* **1974**, *12*, 1.

(27) Gerloch, M.; McKenzie, E. D.; Towl, A. D. C. *J. Chem. Soc. A* 1969, 2850.

(28) Davies, J. E.; Gatehouse, B. M. *Cryst. Struct. Commun.* **1972**, *1*, 115.

Contribution from the Department of Chemistry, Texas A&M University, College Station, Texas 77843

Electronic Structure and Dissociation Energy of the Molybdenum-to-Molybdenum Triple Bond

RANDALL A. KOK and MICHAEL B. HALL*

Received May 20, 1982

Generalized molecular orbital (GMO) and configuration interaction (CI) calculations are reported for the series N_2, P_2, As_2, Sb_2, and Mo_2H_6 in a large Gaussian basis set. Similar calculations are reported for Mo_2H_6 and $Mo_2(NH_2)_6$ in a smaller Gaussian basis set. The potential energy curve for Mo_2H_6 at the GMO–CI level has a minimum at 2.194 Å in excellent agreement with the Mo–Mo distance in a range of systems: $Mo_2(OCH_2CMe_3)_6$ at 2.222 Å, $Mo_2(NMe_2)_6$ at 2.214 Å, and $Mo(CH_2SiMe_2)_6$ at 2.167 Å. By comparing the calculated dissociation energies of the triply bonded diatomics and Mo_2H_6, we predict a dissociation energy for the molybdenum-to-molybdenum triple bond of 284 kJ mol^{-1}. The results indicate the importance of including the differential correlation energy, which in Mo_2H_6 contributes 70 kJ mol^{-1} to the dissociation energy. We find that the larger basis set increases the calculated dissociation energy by 40 kJ mol^{-1}. When we change the hydride ligand of Mo_2H_6 to an amino ligand in $Mo_2(NH_2)_6$, the dissociation energy increases 117 kJ mol^{-1}. A significant fraction of this increase is due to the π-donating ability of the NH_2 ligand, which results in an expansion of the Mo orbitals and a stronger bond. The relationship between the donor strength of the ligand and the expansion of the Mo orbitals may be responsible for much of the variation in the Mo–Mo triple-bond lengths.

Introduction

There has been considerable interest, recently, in determining the bond strengths of metal–metal bonds. Of particular interest are the bond strengths of multiply bonded metal–metal systems and their comparison to those of main-group multiple bonds. For experimental reasons a large fraction of this effort has been directed at determining the strength of the molybdenum-to-molybdenum and tungsten-to-tungsten double or triple bonds.[1-5]

The earliest experimental work was done on $Mo_2(N(CH_3)_2)_6$, for which the enthalpy of formation was accurately measured.[1] However, it was difficult to derive a value for the Mo–Mo triple-bond dissociation energy from this experiment because of the uncertainty in assigning a value for the Mo–$N(CH_3)_2$ bond energy and a formal oxidation state to the metal. The authors suggested a value of 592 ± 196 kJ mol^{-1} for the Mo–Mo triple-bond energy, but the error bars of the value are so large that a useful comparison to main-group bonds is prohibited.

(1) Connor, J. A.; Pilcher, G.; Skinner, H. A.; Chisholm, M. H.; Cotton, F. A. *J. Am. Chem. Soc.* **1978**, *100*, 7738.

(2) Adedeji, F. A.; Cavell, K. J.; Cavell, S.; Connor, J. A.; Pilcher, G.; Skinner, H. A.; Zafarani-Moattar, M. T. *J. Chem. Soc., Faraday Trans. 1* **1979**, *75*, 603.

(3) Hall, M. B. *J. Am. Chem. Soc.* **1980**, *102*, 2104.

(4) Bursten, B. E.; Cotton, F. A.; Green, J. C.; Seddon, E. A.; Stanley, G. G. *J. Am. Chem. Soc.* **1980**, *102*, 4579.

(5) Cavell, K. J.; Connor, J. A.; Pilcher, G.; da Silva, M. A. V. R.; da Silva, M. D. M. C. R.; Skinner, H. A.; Virmani, Y.; Zafarani-Moattar, M. T. *J. Chem. Soc., Faraday Trans. 1* **1981**, *77*, 1585.

0020-1669/83/1322-0728$01.50/0